Numerical Study of Interior Ballistics with Moving Boundary

Hyung-Gun Sung, Sol Park, Gi-Cheol Hong, Tae-Seong Roh, Dong-Whan Choi
Department of Aerospace, Inha University
253 Yonghyun-Dong, Nam-Gu, Incheon, Republic of Korea
tsroh@inha.ac.kr

Keywords: Interior Ballistics, Moving Boundary, Coordinate system

Abstract

The 1-D numerical study of the interior ballistics has been conducted. The unsteady compressible 1-D CFD code using SIMPLER algorithm and QUICK scheme has been developed. The mathematical model of the two-phase flow has been established for the behavior of the interior ballistics. The moving boundary due to the projectile motion as the physical phenomena of the interior ballistics results in the varied control volume. In order to analyze the moving boundary, the numerical codes, which apply the ghost-cell extrapolation method and the Lagrangian method respectively, have been developed. The ghost-cell extrapolation method has been used in the Eulerian coordinate system. The Lagrangian method has been used in Non-Eulerian coordinate system. These codes have been verified through the analysis of the free piston motion problem in the tube. Through this study, the basic techniques of the numerical code for the multi-dimensional two-phase flow of the interior ballistics have been obtained.

1. Introduction

1.1 Interior Ballistics

Solid propellants are normally used in rockets, missiles and cannons. Studies of solid propellants are generally focused on the combustion of the solid rocket motor (SRM). Most of them, however, do not consider the volume change in the combustion chamber of the SRM when the propellant burns. Similarly, in the case of cannon, porosity increases as the propellant burns and the volume increases by the movement of the projectile. In the microscopic view of the cannon chamber before the projectile moves, the increase of porosity can be considered as the volume change. However, the porosity change is not the same as the concept of the moving boundary. Physical phenomenon of the moving boundary occurred by the movement of the projectile is simpler than that of the SRM. The analysis of the interior ballistics of the cannon can be divided into following processes[1-7].

1. Ignition of solid propellants with ignition gas
2. Increase of chamber pressure while burning solid propellants generate gas.
3. Acceleration of the projectile
4. Escape of the projectile from the muzzle

Since the physical phenomena of the interior ballistics are complicated, it is necessary of a numerical code of the multi-dimensional two-phase flow for the analysis. In this study, therefore, the study on the numerical methods used in the code development of the interior ballistics has been performed.

Figure 1 is showing the process of the simplified interior ballistics. In this study, the interior ballistics has been separated in two processes for efficient study shown in Fig. 1. For the numerical study of Process 1 and Process 2, the unsteady compressible 1-D CFD code has been developed. The mathematical model of the interior ballistics has been researched and established. In Process 2, the 1-D codes employed different moving boundary solvers have been developed. The basic techniques for the interior ballistics code have been obtained after combining the two processes.

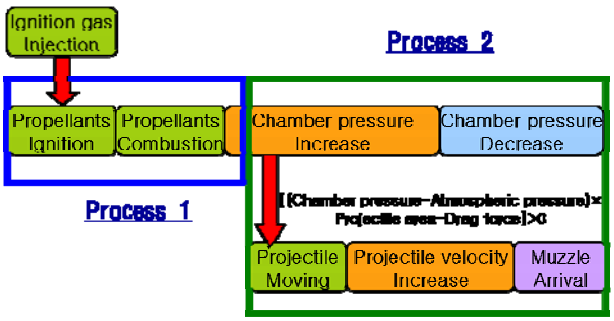

Fig. 1 Process of simplified Interior Ballistics

1.2 Literature Survey

A numerical study of the interior ballistics has been conducted in sequence of the lumped parameter model, one-dimensional two-phase model, and multi-dimensional two-phase model.

Method	Code
Lumped parameter model	IBHVG2, FNGUN
One-dimensional two-phase Model	XKTC, MGBC
Multidimensional two-phase Model	NGEN, TDNOVA

Table 1 Classification of Interior ballistics codes

Table 1 represents various interior ballistics codes. Usually, the lumped parameter model is used to analyze overall performance of canon and to design grain geometry. The 1-D or multidimensional two phase models are used for the study of the ignition or the initial distribution of the propellant in chamber[3].

The Eulerian-Lagrangian method in NGEN code is used to analyze two phase flow. The continuum flow solver which is an explicit method adopts the flux-corrected transport scheme. As the Technique for analyzing moving boundary, the characteristic-based method is used[1,2].

2. Governing Equations

2.1 Two-phase flow in the interior ballistics

The two-phase flow of the interior ballistics is composed of continuous phase of combustion gas and dispersal phase of solid propellants. The interior ballistics has a moving boundary with variable control volume.

In two-phase flow, the solid phase has been calculated by using the Lagrangian-coordinate system. The gas phase has been calculated by using the Eulerian-coordinate system and the Non-Eulerian coordinate system. So each solid and gas phase has been calculated by each coordinate system. In this study, the combustion of solid propellants in the interior ballistics has not been considered. Therefore the governing equations of dispersal phase are not considered either.

The continuity, momentum and energy equations for one dimensional, compressible, unsteady flow are written in conservative form as follows:

Continuity equation,

$$\frac{\delta \rho}{\delta t}+\frac{\delta}{\delta x}(\rho u)=S_C \tag{1}$$

Momentum equation,

$$\frac{\delta \rho u}{\delta t}+\frac{\delta}{\delta x}(\rho u u) = \frac{\delta}{\delta x}\left(\mu \frac{\delta u}{\delta x}\right)-\frac{\delta p}{\delta x}+S_M \tag{2}$$

Energy equation,

$$\frac{\delta \rho h_0}{\delta t}+\frac{\delta}{\delta x}(\rho u h_0) = \frac{\delta}{\delta x}\left(k \frac{\delta T}{\delta x}\right)+\frac{\delta p}{\delta t}+S_E \tag{3}$$

2.2 Projectile motion Equations

The projectile motion equations of all interior ballistics codes are similar each other. The force equilibrium Equation of the projectile in the interior ballistics is

$$m_P a_P=\left(P_B-P_F\right)A_P-F_{Fr}-F_{Drag} \tag{4}$$

In this study, the fraction force and the projectile drag force are neglected because these are not the main contents of this study.

The projectile motion equations are

$$\frac{dV_P}{dt}=a_P \tag{5}$$

$$\frac{dX_P}{dt}=V_P \tag{6}$$

3. Numerical Study

3.1 Numerical method

The CFD code using 1-D finite volume method has been developed for the numerical study of the interior ballistics. The SIMPLER algorithm and QUICK scheme have been used to analyze unsteady compressible flow.

Usually, the method developed for compressible flows is characterized by the use of density as a main variable and extract pressure from the equation of state.

On the other hands, the method with pressure as a main variable usually is used for incompressible flows or low Mach number flows. The CFD code of the interior ballistics takes analysis of compressible flow because the process of the interior ballistics has the increase of density and temperature in the isolated computational domain. The interior ballistics has complex analysis problems such as solid propellant combustion, two-phase flows and moving boundary. Therefore, in this study, the pressure has been taken as the main variable because the pressure-based algorithms are easier than the density based algorithms to solve the problems8).

The modified SIMPLER algorithm has been developed for compressible flows in overall speed range by the study of Karki[9]. So, the modified SIMPLER algorithm has been used for interior ballistics CFD analysis. Figure 2 is the flow chart of the modified SIMPLER algorithm[9].

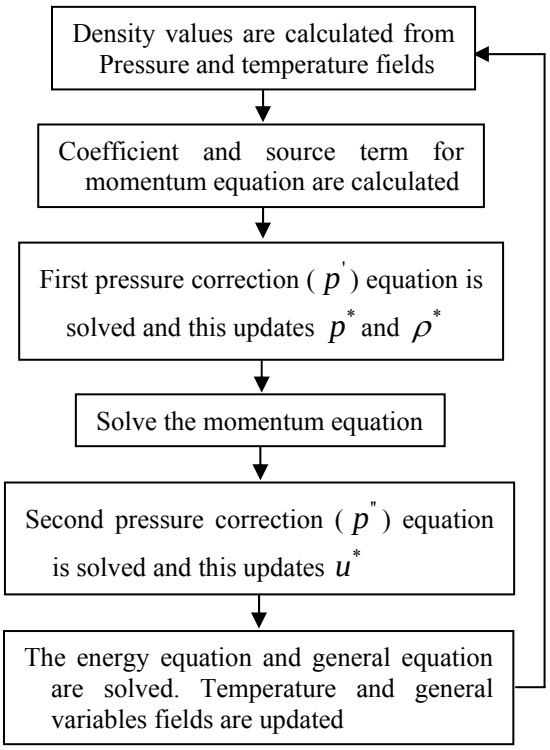

Fig. 2 Flow chart of modified SIMPLER Algorithm

The QUICK scheme has been used to discrete the analysis domain and the fully implicit method has been used for unsteady flow. In this study, the Hayase's QUICK scheme has been used. It can be summarized as follows[10]:

$$\phi_w = \phi_W + \frac{1}{8}\left[3\phi_P - 2\phi_W - \phi_{WW}\right] \text{ for } F_w > 0$$

$$\phi_e = \phi_P + \frac{1}{8}\left[3\phi_E - 2\phi_P - \phi_W\right] \text{ for } F_e > 0$$

$$\phi_w = \phi_P + \frac{1}{8}\left[3\phi_W - 2\phi_P - \phi_E\right] \text{ for } F_w < 0$$

$$\phi_e = \phi_E + \frac{1}{8}\left[3\phi_P - 2\phi_E - \phi_{EE}\right] \text{ for } F_e < 0 \quad (7)$$

3.2 Moving Boundary

Several techniques exist for the moving boundary. These techniques are classified under two main categories by the coordinate system: ① Eulerian-coordinate methods and ② Non-Eulerian coordinate methods10).

The Eulerian coordinate methods employ the fixed grid, and the Non-Eulerian-coordinate methods employ the transformed grid. In moving boundary problem, the Eulerian coordinate methods add or remove the grid cell, and the non-Eulerian-coordinate methods move the grid itself.

The Non-Eulerian coordinate methods are classified under two methods by the grid velocity: ① Lagrangian method ② space conservation law (SCL) method. In the Lagrangian method, the grid velocity is equal to the flow velocity. In the SCL method, however, the grid velocity is not equal to the flow velocity. The Lagrangian method has been used in this study,.

The Eulerian methods are classified by tracking the interface and by calculating the interface value.

In this study, the ghost-cell extrapolation method which assumes that the cell with the moving boundary is a sort of the ghost cell has been used. The ghost cell has been calculated by the extrapolation with the variable values of the nearest cell. Then, the interface between the ghost cell and the nearest cell has been calculated using the variable values of the ghost cell.

3.2.1. Lagrangian method

In the Lagrangian method, each finite control volume of the grid is considered as a lump of gas[11]. Since velocity of the interface of the finite control volume is equal to the flow velocity, the mass of the inflow and the outflow in each control volume is set to be zero. Therefore the 1-D governing equations of the flow are to be ODE form. The mass conservation equation is transformed to the position equation of the interface as

$$\frac{dx_{j\pm\frac{1}{2}}}{dt} = u_{j\pm\frac{1}{2}} \quad (8)$$

So it can calculate the moving interface automatically.

The momentum equation is

$$\frac{d}{dt} m_j \overline{u_j} = P_{j-\frac{1}{2}} A_{j-\frac{1}{2}} - P_{j+\frac{1}{2}} A_{j+\frac{1}{2}} + \overline{P_j}\left(A_{j-\frac{1}{2}} + A_{j+\frac{1}{2}}\right) - \overline{F_{wall}} \quad (9)$$

The energy equation is

$$\frac{d}{dt} m_j \overline{E_j} = P_{j-\frac{1}{2}} A_{j-\frac{1}{2}} u_{j-\frac{1}{2}} - P_{j+\frac{1}{2}} A_{j+\frac{1}{2}} u_{j+\frac{1}{2}} + \overline{q_j} \quad (10)$$

3.2.2. Ghost Cell Extrapolation

To calculate the internal flow, the treatment of the left fixed boundary and the right moving boundary is important.

In this study, both ends of the computational grid have been set as the ghost cells. Each interface between ghost cell and the nearest cell has been calculated by using value of the ghost cell.

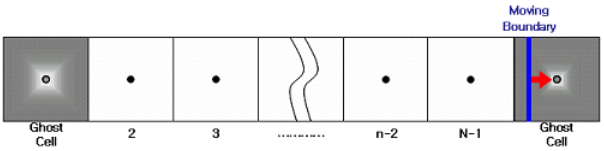

Fig. 3 Free piston model in tube

- **Left ghost cell with fixed boundary**

To calculate impermeable left boundary condition, the value of the left ghost cell is required. The left ghost cell value is as below[12]:

$$\rho_{gh} = \rho_2,\ p_{gh} = p_2,\ u_{gh} = -u_2 \quad (11)$$

u_{gh} is $-u_2$ in equation (11), because the interface between the left ghost cell and the 2nd cell is fixed. The interface value has been obtained by the interpolation of the ghost cell value and the 2nd cell value.

- **Right ghost cell(n cell) with moving boundary by projectile motion**

In the right side of Fig. 3, the moving boundary is in right ghost cell. The projectile has been assumed as the solid wall in right ghost cell. The values of n-1 cell and velocity of the solid wall have been used to obtain the following ghost cell values[13] :

$$\rho_{gh} = \rho_{n-1},\ p_{gh} = p_{n-1},\ u_{gh} = 2V_p - u_{n-1} \quad (12)$$

The interface values between the ghost cell and the n-1 cell have been calculated from the procedure as below; Values of ρ^*, u^*, p^* are obtained from the value of u_{gh} .

If $u_{gh} > u_{n-1}$, values of ρ^*, u^*, p^* sre given by :

$$\rho^* = \rho_{n-1}\left(\frac{p^*}{p_{n-1}}\right)^{1/\gamma}, \quad u^* = V_p, \tag{13}$$

$$p^* = p_{n-1}\left(1-\frac{(\gamma-1)(V_p-u_{n-1})}{2c_{n-1}}\right) \tag{14}$$

If $u_{gh} < u_{n-1}$, values of ρ^*, u^*, p^* are given by :

$$\rho^* = \rho_{n-1}\frac{(\gamma-1)\,p_{n-1}+(\gamma+1)\,p^*}{(\gamma+1)\,p_{n-1}+(\gamma-1)\,p^*} \tag{15}$$

$$u^* = V_p \tag{16}$$

$$p^* = p_{n-1} + \frac{(\gamma-1)\rho_{n-1}(V_p-u_{n-1})^2}{4} \times\left(1+\sqrt{1+\left(\frac{4c_{n-1}}{(\gamma+1)(V_p-u_{n-1})}\right)^2}\right) \tag{17}$$

The interface values have been obtained by following condition,

▪ If $u^* - c^* < 0$ then

$$\rho_{n-1/2} = \rho^*, \quad u_{n-1/2} = u^*, \quad p_{n-1/2} = p^* \tag{18}$$

▪ If $u^* - c^* > 0$ then

$$\rho_{n-1/2} = \rho_{n-1}, u_{n-1/2} = u_{n-1}, p_{n-1/2} = p_{n-1} \tag{19}$$

If $x_p(t+\Delta t)$ which is the position of the solid wall at time $(t+\Delta t)$ remains in right ghost cell of the n-th cell, the overall process repeats again. If the solid wall moves to the n+1st cell, a cell is added to the grid and it becomes a new ghost cell. Also the new ghost cell values are ρ^*, u^*, p^*. The procedure is summarized in the following algorithm:

If $x_p(t+\Delta t) \in n+1$ *Cell* , then

$$[\rho, u, p]^{(t+\Delta t)} = [\rho^*, u^*, p^*]^t \tag{20}$$

and the interface value has been calculated by the same process once again.

4. Test

In order to verify the analysis code of the moving boundary, a free piston motion problem has been used. Figure 4 shows the free piston motion problem[14].

Fig. 4 Free Piston Motion Problem

Table 2 shows the initial conditions of the free piston model. They have been applied to the adiabatic wall. Viscous effects and frictional effects have been neglected. The boundary conditions for the gas slug are that the left-end has zero velocity and the right-end is coupled with the left-end of the piston. The air gas in the free piston problem is assumed to be the calorically perfect gas with the specific heat ratio as 1.4.

Initial Pressure	1.0e+5 (Pa)
Initial Density	1.0 (kg/m³)
Initial Temperature	348.5 (K)
Mass of Piston	0.001 (kg)
Pressure of front of Piston	0.0(Pa)
Diameter of Tube	0.01(m)
Initial Length of Tube	4.0(m)

Table 2 Initial states of Free Piston Model

For the verification of the developed CFD code employed the SIMPLER algorithm and the QUICK scheme, the CFD codes, which apply the verified Godunov and Lax-Wendroff schemes respectively, has been used.

In the Lagrangian method, the approximate Riemann solver and the minmod interpolation method have been used to calculate density, pressure and velocity at the interface. The predicted-corrected scheme has been used for the time integral.

The ghost-cell extrapolation method has been applied to each of the CFD codes; employed the Godunov scheme[12], the Lax-Wendroff scheme[12] and the SIMPLER algorithm with the QUICK scheme. The SIMPLER algorithm has been compared to the Godunov scheme and the Lax-Wendroff scheme. In the Lagrangian method, the number of initial cells is 1000. In the ghost-cell extrapolation method with the Lax-Wendroff scheme and the Godunov scheme, the number of initial cells is also 1000. In the ghost-cell extrapolation method with the SIMPLER algorithm, the number of initial cells is 500. The number of initial cells has been determined by sample tests.

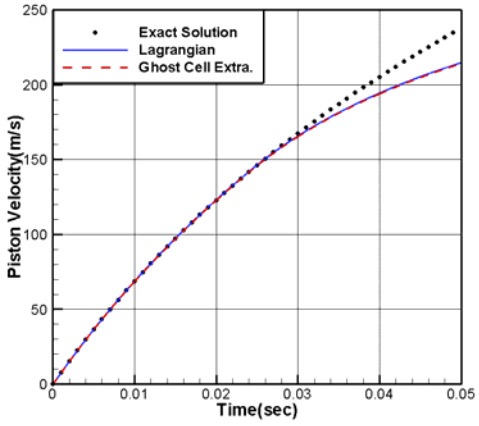

Fig. 5 Velocity as a function of Time for the piston in tube

Figure 5 shows the comparison results of the numerical solutions of the Lagrangian method and the ghost cell extrapolation method with the exact solution from the theory in the reference[14]. Before 0.024sec, there is no difference. The difference after 0.024 seconds between the numerical solutions and the exact solution seems to be generated by theoretical assumptions of the infinite tube and the vacuum in front of piston.

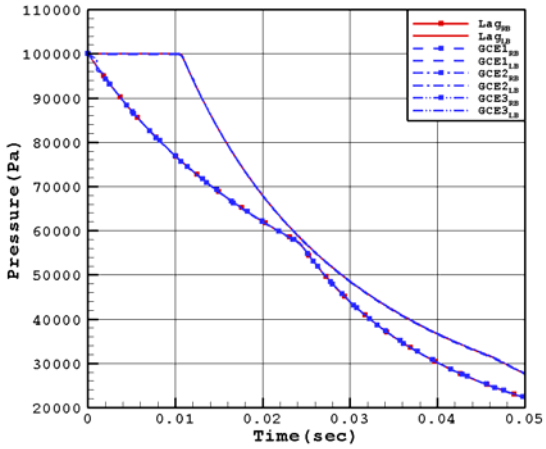

Fig. 6 Pressures as a function of time for both ends in tube

In Fig. 6, the pressure variations with time have been shown at both ends of the tube. The plot named Lag is the result of the Lagragian method. The GCE1 is the result of the ghost-cell extrapolation method employed the SIMPLER algorithm. The GCE2 is the result of the ghost-cell extrapolation method employed the Lax-Wendroff scheme. The GCE 3 is the result of the ghost-cell extrapolation method employed the Godunov scheme. The subscript RB and LB mean the right boundary and the left boundary, respectively. As shown in Fig. 6, there is no quantitative difference in numerical solutions between the Lagrangian method and the ghost-cell extrapolation method.

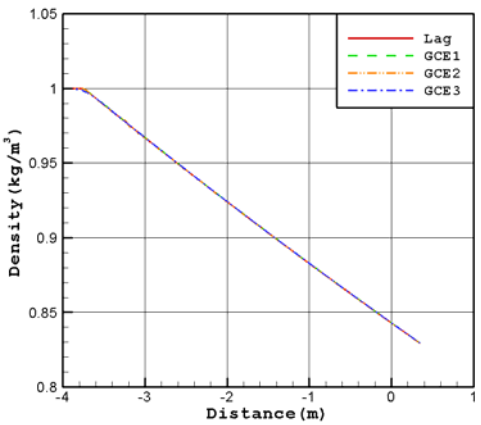

A (0.01sec)

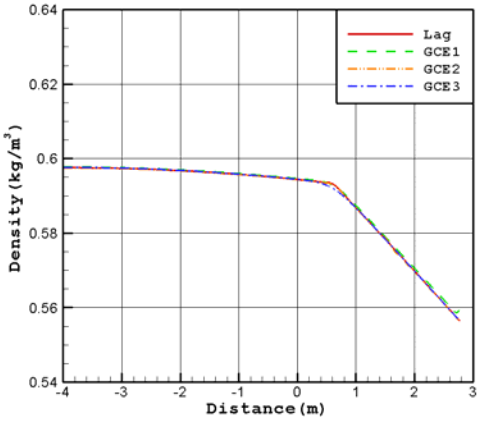

B (0.03sec)

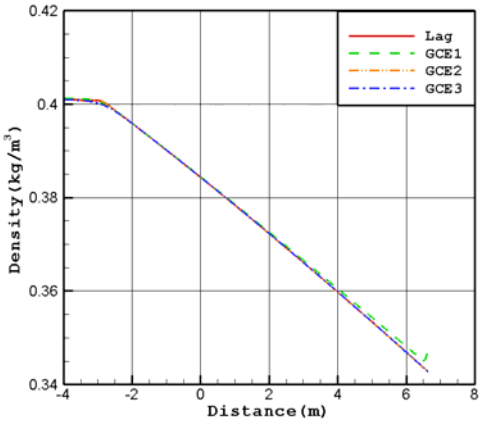

C (0.05sec)

Fig. 7 Distribution of density in tube

Figures 7-A, B and C show the density distribution with time of 0.01sec, 0.03sec, and 0.05sec in the tube. As time goes by, the distance of the piston movement has been increased, and the density distribution has been decreased. And there are no quantitative or qualitative difference in the numerical solution between the SIMPLER algorithm and others of the Godunov scheme and the Lax-Wendroff scheme. As the results, the CFD code employed SIMPLER algorithm has been verified.

Figure 6, 7-A, B and C show that the results of the ghost-cell extrapolation method are quantitatively and qualitatively similar to those of the Lagragian method.

Figure 8 shows the movement of the expansion wave which is generated by the piston movement with time. The solid line named PB represents the pressure behind the piston at each time. The dash dot line named PTube represents the pressure distribution in the tube at each time. The steep descent of pressure shows where the expansion wave exists. Before 0.011sec, the expansion wave has moved to the fixed left boundary. The expansion wave has been reflected at the fixed left boundary. Between 0.011 and 0.024 sec, the reflected expansion wave has moved from the fixed left boundary to the moving right boundary.

After the expansion wave reflected at the fixed left boundary reaches piston, the physical properties of the left side of the piston has been changed steeply. After 0.024 sec, the expansion wave has moved to the fixed left boundary and reflected again. The solid arrows are the path of the movement of the expansion wave.

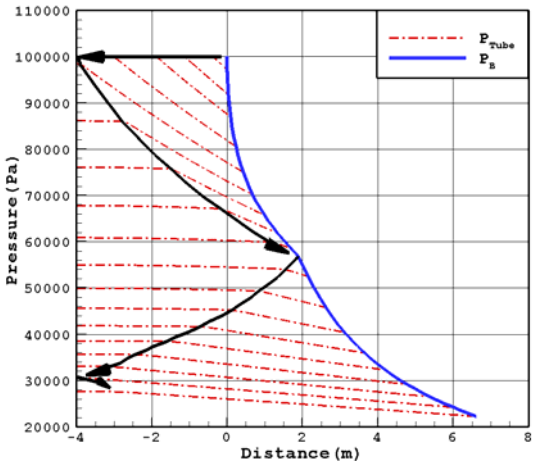

Fig. 8 pressure as a function of time for expansion wave in tube

Conclusion

The 1-D numerical study of the interior ballistics has been conducted. The unsteady compressible 1-D CFD code using SIMPLER algorithm and QUICK scheme has been developed. The mathematical model of the two-phase flow has been established for the behavior of the interior ballistics. The moving boundary due to the projectile motion as the physical phenomena of the interior ballistics results in the varied control volume. For the analysis of the moving boundary, each of the numerical codes with the ghost-cell extrapolation method and the Lagrangian method has been developed. The ghost-cell extrapolation method has been used in the Eulerian coordinate system. The Lagrangian method has been used in Non-Eulerian coordinate system. Each of the developed codes has been verified through the analysis of the free piston motion problem in the tube. As the results, the basic techniques of the numerical code for the multi-dimensional two-phase flow of the interior ballistics have been obtained. The developed codes are going to be used in analysis of the moving boundary occurred by the movement of the projectile in the interior ballistics of the cannon. After combining the code and numerical techniques of solid propellant combustion, a numerical solver for the interior ballistic of the 1-D or multi-dimensional two-phase flow will be developed completely.

References

1) Paul S. Gough: Initial Development of Core Module of Next Generation Interior Ballistic Model NGEN, ARL-CR-234, 1995
2) Michael J. Nusca and Albert W. Horst: Progress in Modeling Ignition in a Solid Propellant Charge for Telescoped Ammunition, ARL-TR-3673, 2005
3) Albert W. Horst and Michael J. Nusca: The Charge Designer's Workbench: A Range of Interior Ballistic Modeling Tools, ARL-TR-3796, 2006
4) Otto K.Heiney and Robert J. West: Interior Ballistics, Muzzle Flash and Gas Gradients of Aircraft Cannon, AFATL-TR-76-34, 1976
5) Frazer-NASH CONSULTAMCY LIMITED: FNGUN User Manual, FNC, 1994
6) H. C. Cho, J. K. Yun, H. D. Shin and C. U. Kim: Prediction of Combustion Field in Granular Propellant with Moving Boundary, KSME Vol. 16 No. 12, 1992, pp.2385~2394
7) Jae-Kun Yoon and Hyung-Soo Hyun: A Study on the Macroscopic Combustion Models of Gun Propellants, KSME Vol. 18, No. 8, 1994, pp.2201~2209
8) S.V. Patankar : Numerical Heat Transfer and Fluid Flow, McGraw-Hill Book Company, 1980
9) K. C. Karki and S. V. Patankar : Pressure Based Calculation Procedure for Viscous Flows at All Speeds in Arbitrary Configurations, AIAA, Vol.27, No. 9, 1989, pp.1167~1174
10) H. K. Versteeg, W. Malalasekera : An Introduction to Computational Fluid Dynamics The Finite Volume Method, Longman, 1995
11) P. A. Jacobs, "Shock Tube Modeling With L1d," The University of Queensland Report 13/98, 1998
12) E. F. Toro : Riemann Solvers and Numerical Methods for Fluid Dynamics. A Practical Introduction, Springer-Verlag, Berlin, 1997
13) A. Chertock, A. Kurganov : A Simple Eulerian Finite-Volume Method for Compressible Fluids in Domains with Moving Boundaries, submitted to Communications in Mathematical Sciences, 2007
14) R. E. Berggren, R. M. Reynolds, 'The Light-Gas-Gun Model Launcher', NASA-Ames Research Center, 1965

Acknowledgement

Authors are gratefully acknowledging the support by Defense Acquisition Program Administration and Agency for Defense Development.

Appendix

Nomenclature

A_P	Area of projectile base (m^2)
a_P	Acceleration of projectile (m/s^2)
c	Speed of sound (m/s)
F_{Drag}	Drag force (N)
F_{Fr}	Friction force (N)

F_{wall} Shear friction force at wall (N)
h_0 Total enthalpy (J/kg)
k Thermal conductivity (W/m·K)
m_P Mass of projectile (kg)
p Pressure (Pa)
q Rate of heat transfer into cell
S_C Source of continuity equation
S_M Source of momentum equation
S_e Source of energy equation
V_P Velocity of projectile (m/s)
X_P Location of projectile in x-axis (m)
γ Specific heat ratio
μ Viscosity (N·s/m^2)
ρ Density (kg/m^3)

Subscript

gh Ghost cell
B Base or back of projectile
F Front of projectile

Superscript

* Interface between n-1 cell and ghost cell